

A Study of Temperature Effect on Vertically Aligned Carbon Nanofibers for Bio/Chemical Sensors Development

Siva Naga Sandeep Chalamalasetty¹, Uchechukwu C. Wejinya^{2,*}, *Member, IEEE* and Zhuxin Dong², *Student Member, IEEE*.

¹Department of Microelectronics and Photonics, University of Arkansas, Fayetteville AR 72701, USA

²Department of Mechanical Engineering, University of Arkansas, Fayetteville, AR 72701, USA

*Corresponding Author: E-mail: uwejinya@uark.edu

Abstract—One of the major limitations in the development of ultrasensitive electrochemical biosensors based on one dimensional nanostructure is the difficulty involved with reliably fabricating nanoelectrode arrays (NEAs). In this work, to ensure nanoelectrode behavior and higher sensitivity, Vertically Aligned Carbon Nano Fibers (VACNF) are precisely grown on 100 nm Ni dots with 1 μ m spacing on each micro pad. However, in order to examine the quality and measure the height and diameter of the VACNFs, a surface detection and measurement tool at the nanoscale level is employed. In this paper, we introduce an approach to measure these nano-scale features through Atomic Force Microscope (AFM). With this method, both the 2D and 3D images of sample surface are generated and the sizes of carbon nanofibers are obtained with statistical analysis. Furthermore, temperature effect on the dimensions of VACNFs is studied.

I. INTRODUCTION

It has been known for over a century that filamentous carbon can be grown by catalytic decomposition of a carbon source onto a metal surface. In a US patent published in 1889 [1], it is narrated that carbon filaments are grown from carbon containing gases using an iron crucible. Despite of the high probability that this early material is a carbon nanofiber and due to the lack of appropriate tools to verify this observation, scientists waited until the invention of high resolution microscope to verify the observation. Research works through the 1950s have shown that filamentous carbon can be grown onto a heated metal surface using a variety of hydrocarbons, other gases and metals the most effective of which were the iron, cobalt and nickel. In 1985, Buckminster fullerene C₆₀ was discovered by team headed by Kroto [2] followed by the illustration of Iijima [3] that carbon nanotubes are formed during arc discharge synthesis of C₆₀. Throughout the evolution, detection of diseases and their causing pathogens have become a big challenge for the researchers. Initially, researchers used to rely on indicator organisms for predicting the disease. But with the increase in awareness of the diversity exhibited by microbes, researchers have concluded that use of indicator organism is no more a safe practice for quantification [4]. Thus the need for fast, reliable, ultrasensitive, portable and automated devices has increased. Newer methods involving immunofluorescence techniques and nucleic acid analysis

provide valuable opportunities for rapid and more specific analytical methods. Particularly, electrochemical (EC) biosensors are attractive for detecting a wide range of species, including proteins, nucleic acids, small molecules and viruses because of their relative simplicity, portability, low cost and low power requirement. EC biosensors consist of two primary components: a recognition layer containing a biomolecule and an electrochemical signal transducer. They make use of electrochemical reactions or the surface property changes upon target binding. Advances in microfabrication technology have provided electrode configurations such as microelectrode arrays [5] and interdigitated arrays (IDA) [6], but their performance can be further enhanced by miniaturizing to nanoscale. Recent progress in nanofabrication technologies like electron beam lithography and nanoimprinting enable fabrication of one-dimensional nanostructure electrodes, like carbon nanofibers [7-9], carbon nanotube bundles [10-11], nanoscale IDA [12], silicon nanowires [13] and diamond nanowires [14], which are capable of high spatial and temporal resolutions, possibly yielding sufficient sensitivity to single molecule detection. Among various types of one-dimensional nanoscale electrodes, vertically aligned carbon nanofibers (VACNFs) have received tremendous attention because of their attractive properties such as high electrical and thermal conductivities, superior mechanical strength, a wide electrochemical potential window, flexible surface chemistry and biocompatibility [15-16]. One hindrance in miniaturization of devices based on VACNFs is their inability to grow uniformly. After the first successful development of carbon nanofibers, many researchers have proposed and grown the fibers using different techniques. Of these, catalyst enhanced Plasma Enhanced Chemical Vapor Deposition (PECVD) is the most common. Yet the methods need refinement in order to grow fibers of uniform shape and size. With an increase in the number of ways that are available for the fabrication of Vertically Aligned Carbon Nanofibers (VACNFs), the need for the advanced microscopic analysis tools has increased. From a close look into the fabrication methodologies, one can conclude that carbon nanofibers are produced in the extreme temperatures. Hence it is of prime importance to understand how the carbon nanofibers behave at variable temperatures. This is also an important aspect because the main hindrance in

many instruments being unsuccessful in the market is their variation in their performance to the ideal conditions and in real time. This is because in lab conditions the equipment is always tested in around room temperature which in general doesn't hold in the real world thus making them unsuccessful at commercialization. For VACNFs we believe that sensitivity is directly dependent on its height and diameter. Thus this study is conducted to test whether the changes in temperature will have any significant effect on VACNFs' dimensions.

The relationship between the nanoparticle diameter to its surface and bulk temperature is given by Gregory Guiliber [17] as follow:

$$\frac{T_x}{T_{x,\infty}} = \left(1 - \frac{\alpha}{D}\right)^{S-\frac{1}{2}} \quad (1)$$

Where, T_x is surface temperature, $T_{x,\infty}$ is bulk temperature, α is height, D is diameter and S is spin number. A regression line equation is developed from the lab experiments using Taguchi's approach [18] and then compared with Guiliber's equation to see if the experimental results are in accordance with theory.

II. ATOMIC FORCE MICROSCOPY

Atomic Force Microscope (AFM) is a very high resolution type of scanning probe microscope that has resolution of fractions of a nanometer. The AFM was created specifically to generate a three-dimensional view of a scanned object, unlike the Scanning Electron Microscope (SEM) that can only produce two dimensional views. With the ability to scan almost any type of surface, the AFM is used in many types of research. Surfaces include polymers, ceramics, composites, glass, and biological samples. The AFM also has a variety of operation modes including contact mode, lateral force microscopy, noncontact mode, tapping mode, and phase imaging. The microscope uses a micro scale cantilever with a probe at the end that is used to scan a surface. A beam deflection system consisting of a laser and photo detector is built into the microscope to measure the position of the beam and ultimately the position of the cantilever tip. The laser beam is placed on the cantilever tip and the beam deflection measures the displacement the sample exerts on the cantilever. The spring constant is known based on what type of scanning probe is used. With its three dimensional capabilities and ability to operate in air rather than a vacuum sealed environment, the Atomic Force Microscope aids many studies in biological macromolecules, tribology, optical and imaging sciences. The microscope has the capabilities of scanning living organisms through the study of measurements of protein-ligand interactions on living cells and many other research applications. The atomic force microscope has been used as the primary tool for direct measurement of interatomic force gradients, detection and localization of single molecular recognition events, single molecule experiments at the solid-liquid interface and fractured polymer/silica fiber surface

research. Owing to the advantages stated above, AFM is capable of completing the dimensional analysis of the nano fibers and cavities.

III. FABRICATION OF NANO ELECTRODE ARRAY CHIPS

The intensively sensitive fabrication process of vertically aligned carbon nanofibers (VACNFs) nano electrode arrays (NEAs) includes six major steps done on a four inch silicon (100) wafer that is previously coated with 500 nm of silicon dioxide. The steps of the fabrication process of both Unetched and etched are shown in Fig. 1. The steps include A) metal deposition; (B) Nano-patterning of Ni catalyst dots; (C) directional growth of CNFs; (D) silicon dioxide deposition for electrical isolation and mechanical support; (E) chemical mechanical polishing (CMP) to expose CNF tips and (F) a wet etch with 7:1 HF.

A. Deposition of Metal

Electron beam evaporation is used to deposit a 200 nm thick Cr film and then the wafer is immersed in acetone for one hour. Once removed from the acetone, the wafer is sprayed with methanol and isopropyl alcohol and blown dry with N₂.

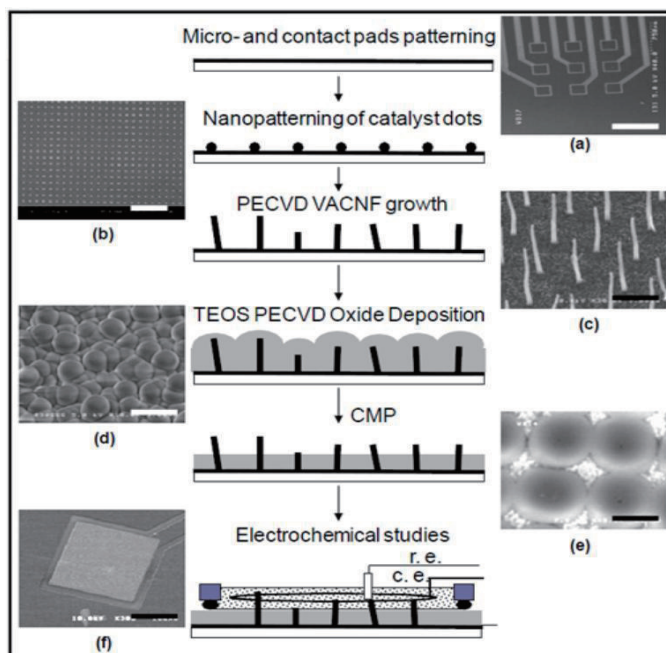


Fig. 1. The procedure of fabricating biosensors based on nanopatterned VACNFs: (a) deposition of metal; (b) nanopatterning; (c) growth of CNFs; (d) deposition of silicon dioxide; (e) chemical mechanical polishing; (f) electrochemical characterization.

B. Growth of CNFs

The next step is growing the VACNFs on the nickel dots that were created in step B. The growth is DC-biased PECVD growth. At a processing pressure of 6.3 mbar, plasma power of 180W and 700 degrees Celsius, 125sccm C₂H₂ feedstock and 444sccm NH₃ diluents were initiated. Then a five minute thermal annealing at 600 degrees Celsius is carried out

following with 250 sccm NH_3 . To attain the growth temperatures and thermal anneal needed, a 60 degree Celsius per minute incline was used. Each individual CNF vertically arranged to freely stand on the surface with Ni catalyst on each tip. To check and affirm the process was done correctly, a fifteen minute deposition was conducted. The average results included a height of 1.5 microns, 100 nanometer base diameter and 70 nanometer tip diameter. The uniformity of the growth was then checked by SEM.

C. Deposition of Silicon Dioxide

PECVD of silicon dioxide is managed next. To passivate the sidewalls of each individual fiber, a 3 micron SiO_2 layer was deposited onto the wafers using a pressure of 3Torr, temperature of 400 degrees Celsius and RF power of 1000W. The process included a parallel plate, dual RF, PECVD using a mixture of 6000 sccm of O_2 and 2-3 ml/min of tetraethylorthosilicate (TEOS). A highly conformal coating of SiO_2 was created on the newly created fibers and interconnects.

D. Chemical Mechanical Polishing

By CMP, existing of stock removal and final polish, the overrun oxide and a portion of the VACNF's are removed. This process involved removing the existing material with 0.5 m alumina (pH 4) at 10 ml/min, 60-rpm platen, 15-rpm carrier, and 15 psig down force at 150nm/min. A 0.1_m alumina (pH 4) at 10 ml/min, 60-rpm platen, 15-rpm carrier, and 25 psig down force was operated for final polish at 20nm/min. The wafer was cleaned by immersing it into a solution composed of water, hydrogen peroxide, and ammonium hydroxide at a ratio of 80:2:1 respectively and then spin-dried. The aim to re-expose the VACNF tips was carried out as well as planarization of the surface

IV. EXPERIMENTAL SETUP

Fabricated chips are now subjected to variable temperatures at a constant humidity and changes in the dimensions of the fiber are recorded. Taguchi's method of statistical analysis is used for the evaluation of the nanofiber dimensional changes with temperature. In this method, a chip is taken and placed in the Environmental chamber (Manufactured by Cincinnati Sub Zero model No. MCBH 1.3) after attaining the required temperature and Constant relative humidity of 10%. They are held there for 30 minutes then cooled down back to the room temperature of 23°C. The chips are then treated in the dry box to bring down the humidity to less than 1% and the dimensions are measured using the AFM.

In order to accurately determine the height and diameter of the VACNFs before and after treating in the environmental chamber, an Atomic Force Microscope is employed. The AFM used in the experiment is the Agilent 5500-ILM highly sensitive microscope shown in Fig. 2. The scanning and characterization is done under Acoustic AC (tapping) imaging mode as shown in Fig. 3. The AFM probe utilized during imaging has a resonant frequency of 190 kHz and a spring

constant of 48 N/m. As introduced in the AFM specification, during intermittent contact, the tip is brought close to the sample so that it lightly contacts the surface at the bottom of its travel, causing the oscillation amplitude to drop. Hence, we may completely ignore the influence of the cantilever tip during the size measurement as it cannot change anything of the target shape without contacting. It is important to note that the VACNFs are not electrochemically treated.

As shown in Fig. 2, the sample chip containing nine electrode arrays after treating in the environmental chamber will be placed over the target holder and is placed in the microscope for scanning. By using a light microscope, we tried to see the surface over the unetched and etched substrate. The surface looks like as shown inset of Fig. 2.

As shown in the Fig. 3, as the tip touches the surface, there will be a change in the frequency of the wave. Computer software records the changes in wavelength and converts it to real time surface topography.

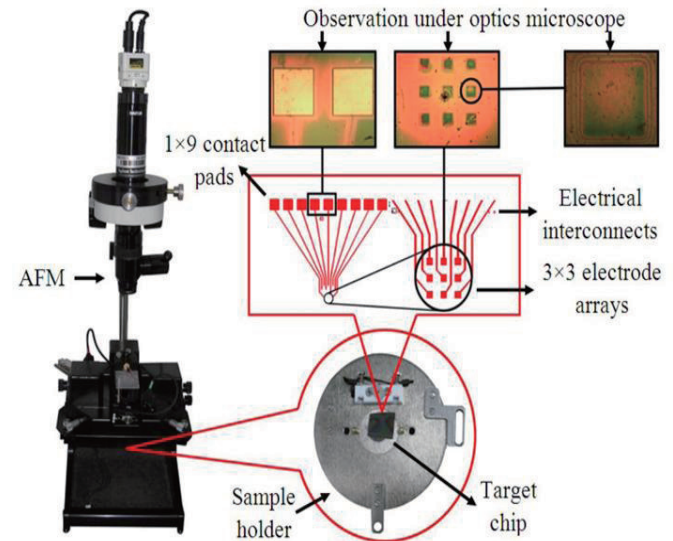


Fig. 2. AFM-based experimental setup showing the sample holder and chips for scanning and characterization.

V. EXPERIMENTAL RESULTS

A. Scanning and Measurement

Before measuring the size of VACNFs and cavities their location should be found out. Thus, we scan a $5\ \mu\text{m} \times 5\ \mu\text{m}$ square area in the middle of the chip. After locating the fibers in the scanned area, we zoom into a $2\ \mu\text{m}$ square area, which encloses the identified nanofiber tips and cavities. to obtain clear scan image and guarantee a better and more accurate measurement. When a fiber appears clear in a scan topography image, a straight line is drawn in any direction in the 2-dimensional topography image to cross the target. At the same time, we obtain the vertical information along the line to complete a measurement. This procedure is repeated until

adequate amount of data is collected before starting on another array.

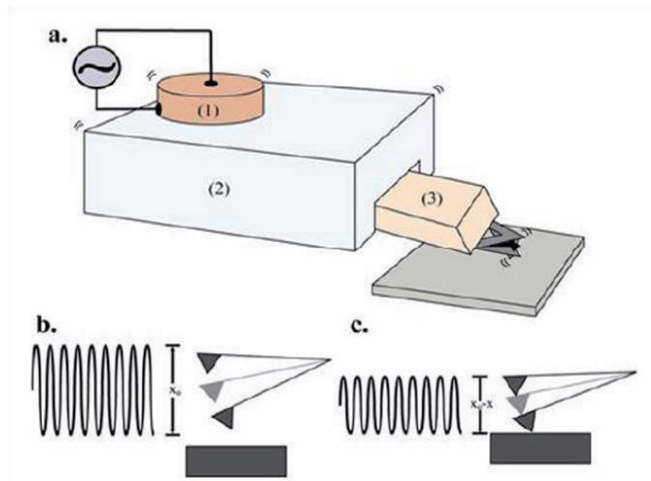


Fig. 3. AFM probe motion under Acoustic AC Mode: a. (1) AC applied to the nose cone; (2) the base body of the cantilever beam; (3) the cantilever beam with its tip; b. & c. the cantilever driven to oscillate in sinusoidal motion.

A 2-D cross section image of roughly $5\ \mu\text{m}$ square area is shown in Fig. 4. Patterned carbon nanofibers are clearly visible in the figure. After having a clear view of the fibers, we zoom in the scan area to get a better view of the fibers by zooming into a scan area of approximately $2\ \mu\text{m}$ square as shown in Fig. 5. For the measurement of dimensions (height and diameter) of each fiber is carried out by drawing a linear line across the fiber to get a graphical 2-D image. The cross section line drawn for measurement of the nanofibers is shown in Fig. 6. As shown in Fig. 6, the horizontal line indicates the diameter of the nanofiber while the vertical line indicates the height of the nanofiber.

Fig. 7 shows a clear 3-D image from the 2-D image. It provides a better understanding of the material characteristics.

To ensure the accuracy, ten readings are recorded for each of the nine nanoelectrode array and then the average of 90 readings is calculated. In this way, the results are precise and accurate. A table containing the average values of diameter and height of nanofibers at each different temperature and humidity is shown in Table I.

B. Result Discussion

From the table it is clear that the nanofiber dimensions change with changes in temperature. As per the theory, material contracts with decrease in the temperature and therefore we can expect an increase in height and decrease in the diameter simultaneously. Conversely, the diameter increases with the increase in the temperature and height

decreases.

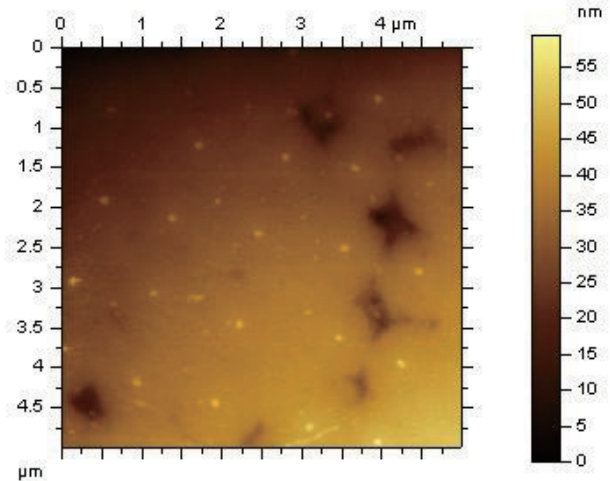


Fig. 4. A 2-D cross section image from the AFM showing the patterned CNF. Cross section area is $5\ \mu\text{m} \times 5\ \mu\text{m}$.

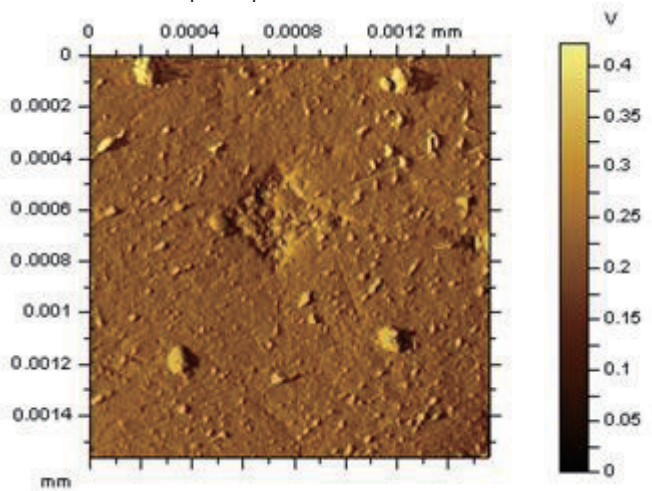


Fig. 5. A 2-D cross section image from the AFM showing the patterned CNFs. Cross section area is $1.2\ \mu\text{m} \times 1.4\ \mu\text{m}$.

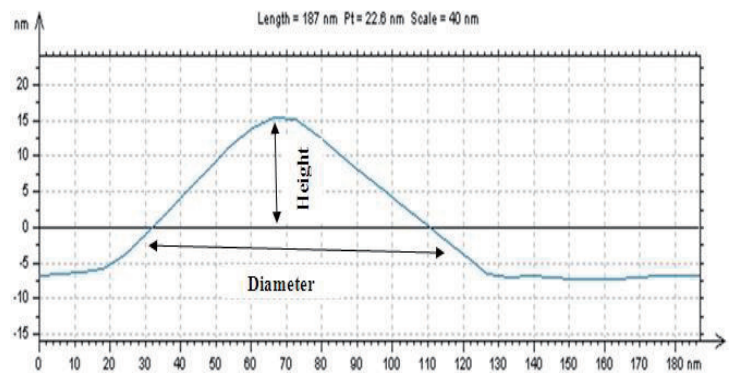


Fig. 6. Cross section information for measurement based on line crossing.

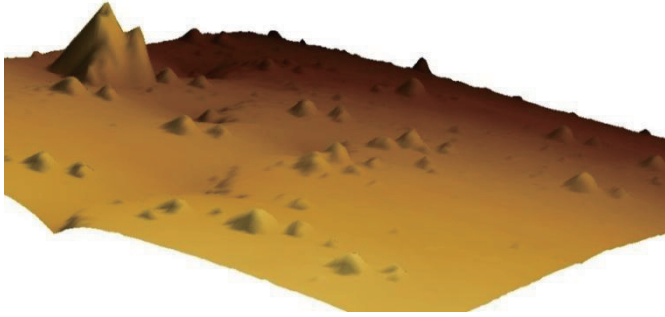


Fig. 7. A 3-D cross section image from the AFM showing the patterned CNFs. Cross section area is $1.2\mu\text{m} \times 1.4\mu\text{m}$.

The results are in accordance with the theory. A graph plotted on nanofiber height with changes in the temperature is shown in Fig. 8. It is clearly evident from the regression line equation that there is a decline in the height of the nanofiber with increase in temperature as it has a negative slope. Conversely, an increase in diameter of the nanofiber is observed with the increase in the temperature as shown in Fig. 9. with a line of positive slope. These results are in complete accordance with the theory.

TABLE I: AVERAGE DIAMETER AND HEIGHT OF THE CARBON NANOFIBERS AT DIFFERENT TEMPERATURES AND CONSTANT HUMIDITY.

Temperature (°C)	Humidity (%)	Average diameter (nm)	Average height (nm)
-10	10	136.89	6.02
0	10	136.98	8.39
5	10	140.98	8.88
10	10	127.11	9.29
15	10	136.64	9.84
20	10	139.02	10.12
25	10	144.36	8.90
30	10	115.76	7.15
35	10	136.14	7.38
40	10	144.79	5.52
45	10	142.27	8.72
50	10	154.48	6.83
55	10	129.26	5.69
60	10	147.32	4.65
65	10	133.74	5.77
70	10	140.34	8.79
75	10	141.65	8.45
80	10	153.10	7.60
85	10	151.48	8.32
90	10	156.02	8.77

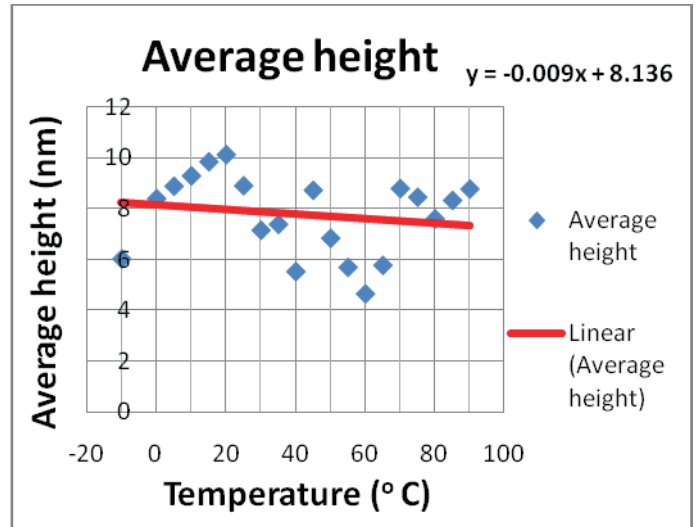


Fig. 8. Nanofiber height plotted against temperature.

C. Statistical Analysis

Confidence Interval

For the experiments like these with high data acquisition, statistical analysis is of pivotal importance. In statistics, a confidence interval (CI) is an interval estimate of the overall population. It would help us define the population more accurately by defining them by a range which includes the mean of the population. This in general is calculated based on the mean and standard deviation of the population. The range varies based on the percent of the population that should be included. In general for a huge data, 95% population inclusion will be a very good estimate. Hence we calculate the confidence interval for 95% population following equation (2) for calculating the confidence intervals.

$$CI = [\bar{X} - Z \times \frac{\sigma}{\sqrt{N}}, \bar{X} + Z \times \frac{\sigma}{\sqrt{N}}] \quad (2)$$

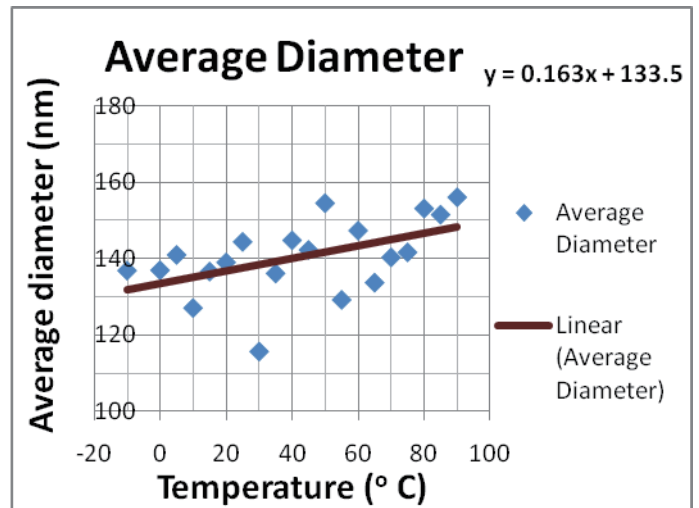


Fig. 9. Nanofiber diameter plotted against temperature.

ACKNOWLEDGMENT

Where, \bar{X} is the mean values of the samples; Z, the critical value, is equal to 1.96 in a 95% CI; σ is the standard deviation and N is the number of the samples which is equal to 90 in this case. Detailed confidence interval for each temperature is given in Table II. A sample calculation is shown below. For instance at temperature of -10 °C, the average diameter is 136.89 nm while the average height is 6.02nm. And their standard deviations are 7.73nm and 0.69nm respectively. Now using the Z-value of 1.96, we can calculate substituting the values in equation (2). Thus the confidence interval will be $\{136.89 - 1.96 \times 7.73/90^{0.5}, 136.89 + 1.96 \times 7.73/90^{0.5}\}$. Thus we attain the confidence interval for the inclusion of 95% population.

From the confidence interval data, it is clearly evident that all the data acquired for a particular temperature falls very close as the range is very short indicating the accuracy of the microscope. As the average is of 90 measurements we are sure that the values are precise and accurate.

TABLE II: CONFIDENCE INTERVALS OF DIAMETER AND HEIGHT AT DIFFERENT TEMPERATURES.

Temp (°C)	Diameter CI		Height CI	
	LB	UB	LB	UB
-10	135.29	138.49	5.88	6.16
0	135.09	138.86	8.26	8.52
5	138.12	143.85	8.62	9.14
10	126.62	127.60	9.07	9.51
15	135.21	138.07	9.54	10.14
20	136.63	141.41	9.76	10.48
25	142.77	145.95	8.67	9.13
30	115.06	116.46	7.01	7.29
35	135.00	137.28	7.23	7.53
40	143.95	145.62	5.39	5.66
45	141.04	143.51	8.51	8.93
50	153.47	155.49	6.67	7.00
55	127.26	131.26	5.60	5.77
60	146.16	148.49	4.52	4.77
65	130.29	137.19	5.55	5.98
70	138.71	141.96	8.59	8.99
75	139.57	143.72	8.22	8.68
80	149.82	156.37	7.45	7.75
85	148.92	154.04	8.11	8.53
90	151.11	160.93	8.43	9.10

CI indicates confidence Interval. LB, UB indicates Lower and Upper Boundaries respectively. All dimensions are in nm.

The authors would like to express their sincere gratitude to Dr. Meyya Meyyappan of NASA AMES research center for providing us with the fabricated nanoelectrode chips and for his timely support.

REFERENCES

- [1] .V. Hughes and C. R. Chambers, *Manufacture of Carbon Filaments*, US Patent No. 405, 480, (1889).
- [2] W. Kroto, J. R. Heath, S. C. O'Brien, R. F. Curl, and R. E. Smalley, *Nature (London)* **318**, 162 (1985).
- [3] S. Iijima, *Nature (London)* **354**, 56 (1991).
- [4] National Research Council and Committee on Indicators for Waterborne Pathogens, 2004. *Indicators for Waterborne Pathogens*. National Academies Press, Washington, DC.
- [5] K. Dill, D. D. Montgomery, A. L. Ghindilis, K. R. Schwarzkopf, S. R. Ragsdale and A. V. Oleinikov, "Immunoassays based on electrochemical detection using microelectrode arrays : Microarrays for Biodefense and Environmental Applications" 2004. *Biosens. Bioelectron.* 20, 736-742.
- [6] O. Niwa and H. Tabei, "Voltammetric Measurements of Reversible and Quasi-Reversible Redox Species Using Carbon Film Based Interdigitated Array Microelectrode", 1994. *Anal. Chem.* 66(2), 285-289.
- [7] J. Li, J. Koehne, A. M. Cassell, H. Chen, Q. Ye, H. T. Ng, J. Han and M. Meyyappan, "Miniaturized Multiplex Label-Free Electronic Chip for Rapid Nucleic Acid Analysis Based on Carbon Nanotube Nanoelectrode Arrays", 2004a. *J. Mater. Chem.* 14, 676-684.
- [8] J. Li, J. Koehne, A. M. Cassell, H. Chen, Q. Ye, H. T. Ng, J. Han and M. Meyyappan, "Bio-Nano Fusion in Sensor and Device Development", 2004b. *MCB I* (1), 69-80.
- [9] M. A. Guillorn, T. E. McKnight, A. Melechko, V. I. Merkulov, P. F. Britt, D. W. Austin, D. H. Lowndes and M. L. Simpson, "Individually Addressable Vertically Aligned Carbon Nanofiber Based Electrochemical Probes", 2002. *J. Appl. Phys.* 91 (6), 3824-3828.
- [10] P. He and L. Dai, "Aligned Carbon Nanotube-DNA electrochemical Sensors", 2004. *Chem. Commun.*, 348-349.
- [11] Y. H. Yun, V. Shanov, M. J. Schulz, Z. Dong, A. Jazieh, W. R. Heineman, H. B. Halsall, D. K. Y. Wong, A. Bange, Y. Tuf and S. Subramaniam, "High Sensitivity Carbon Nanotube Tower Electrodes", 2006. *Sens. Actuators B* 120, 298-304.
- [12] P. V. Gerwen, W. Laureyn, W. Laureys, G. Huyberechts, M. O. D. Beeck, K. Baert, J. Suls, W. Sansen, P. Jacobs, L. Hermans and R. Mertens, "Nanoscaled Interdigitated Electrode Arrays for Biochemical Sensors", 1998. *Sensors and Actuators B*, vol. 49, 73-80.
- [13] F. Patolsky, G. Zheng and C. M. Lieber, 2006. "Fabrication of Silicon Nanowire Devices for Ultrasensitive, Label-Free, Real-Time Detection of Biological and Chemical Species", *Nat. Protocols* 1, 1711-1724.
- [14] N. Yang, H. Uetsuka, E. Osawa and C. E. Nebel, "Vertically Aligned Diamond Nanowires for DNA Sensing", 2008. *Angew. Chem. Int. Ed.* 47, 5183-5185.
- [15] J. Li and M. Meyyappan, 2004. *Carbon Nanotubes: Science and Applications*. CRC Press, Boca Raton, FL.
- [16] A. V. Melechko, V. I. Merkulov, T. E. McKnight, M. A. Guillorn, K. L. Klein, D. H. Lowndes and M. L. Simpson, 2003. "Large-Scale Synthesis of Arrays of High-Aspect-Ratio Rigid Vertically Aligned Carbon Nanofibers". *Nanotechnology* 14(2003), 1029-1035.
- [17] G. Guisbiers and L. Buchailot, "Universal Size/Shape-Dependent Law for Characteristic Temperatures, 2009, *Physics Letters A*, 374:305.
- [18] Ravella Sreenivas Rao, C. Ganesh Kumar, R. Shetty Prakasham, Dr. Phil J. Hobbs "The Taguchi methodology as a statistical tool for biotechnological applications: A critical appraisal" *Biotechnol. J.* 2008, 3, 510-523; DOI 10.1002/biot.200700201.